CROATICA CHEMICA ACTA CCACAA **71** (4) 929–948 (1998)

ISSN-0011-1643
CCA-2540 *Original Scientific Paper*

Evidence of the »Memory« Effect of Amorphous Aluminosilicate Gel Precursors by Simulation of Zeolite Crystallization Processes Using the Population Balance Method

*Tatjana Antonić and Boris Subotić**

Ruđer Bošković Institute, Bijenička 54, P. O. Box 1016, 10001 Zagreb, Croatia

Received January 20, 1998; accepted September 17, 1998

There is abundant experimental evidence that most, or even all zeolite nuclei are formed in the aluminosilicate gel and/or gel/liquid interface by a linking of specific subunits during gel precipitation and/or ageing. Since the nuclei (particles of quasicrystalline phase) cannot grow inside the gel matrix, they start to grow after being »released« from the gel dissolved during the crystallization, *i.e.* when they are in full contact with the liquid phase (autocatalytic nucleation). Based on these findings it was assumed that the rate of autocatalytic nucleation depends on the rate of gel dissolution as well as on the number and distribution of nuclei in the gel matrix, but that crystal size distribution in the crystalline end product depends exclusively on the number and distribution of nuclei in the gel matrix and not on the crystallization conditions, or even on the treatment of aluminosilicate gel precursor prior to crystallization. This so called »memory« effect of amorphous aluminosilicate precursors was evidenced by simulation of zeolite crystallization under different conditions, using the population balance method.

This article is dedicated to Professor Egon Matijević on the occasion of his 75th birthday.

* Author to whom correspondence should be addressed. (E-mail: subotic@rudjer.irb.hr)

INTRODUCTION

A typical hydrothermal crystallization of zeolites includes precipitation of an amorphous aluminosilicate precursor (gel), by mixing together alkaline aluminate and silicate solutions, and transformation of the precipitated gel to crystalline phase(s) by heating the reaction mixture (particles of precipitated gel dispersed in supernatant) at elevated temperature.[1–3] Transformation of an amorphous aluminosilicate gel to zeolite(s) is a solution-mediated process[4–9] that occurs through a chain of interdependent events: (i) dissolution of amorphous aluminosilicate precursor in hot alkaline solution, (ii) saturation (with respect to the precursor) and supersaturation (with respect to zeolite), respectively, of the liquid phase with reactive aluminate, silicate and/or aluminosilicate species, and (iii) formation of primary zeolite particles (nucleation) and their growth from the supersaturated solution. Since the solubility of gels is 2–4 times higher than the solubility of zeolites,[4,7,9–12] the gel is a »resorvoir« of reactive aluminate, silicate and aluminosilicate species needed for nucleation and crystal growth of zeolites; the reactive species are transferred from the gel, through the liquid phase, to the growing zeolite particles (crystals) until the entire amount of gel is dissolved and transformed to zeolite(s).

In spite of more than four decades of research and progress in zeolite synthesis techniques and experience, there is still much uncertainty regarding the relevant mechanisms of zeolite nucleation and crystal growth. Various nucleation mechanisms, such as homogeneous,[13–16] heterogeneous,[7,17,18] and secondary nucleation[13,19,20] in the liquid phase supersaturated with soluble aluminate, silicate and aluminosilicate species as well as a nucleation process on the gel/liquid interface[21] have been proposed as the processes responsible for the formation of primary zeolite particles. Crystallization of various types of zeolites from clear aluminosilicate solutions[14,22–26] undoubtedly demonstrated that nucleation may occur in the liquid phase in the absence of a solid precursor (gel). Homogeneous nucleation[10,13–16] was frequently assumed as a possible process of formation of nuclei in the liquid phase. However, the analysis of the kinetics of homogeneous nucleation of zeolites A and Y showed that the rate of homogeneous nucleation is extremely slow;[27] this excludes homogeneous nucleation in the liquid phase as a process responsible for the formation of zeolite primary particles. Also, some effects observed during the crystallization of zeolites from amorphous aluminosilicate precursors (gels), for instance the increasing rate of nuclei formation (autocatalytic nucleation),[5,7–9,17,21,22,28] a large portion of fine particles in the crystalline end product,[7,29] the influence of gel ageing on the crystallization process,[7,28,30–33] and bimodal particle size distribution in the crystalline end products[5,7,9,22,34,35] cannot be readily explained only by the

classical approaches to the formation of primary zeolite particles in the liquid phase (homogeneous, heterogeneous and secondary nucleation). On the other hand, there is abundant experimental evidence that a considerable part of nuclei are formed in the gel and/or at the gel/liquid interface by linking of specific subunits during gel precipitation and/or ageing.[5,27,33,36–42] Furthermore, recent evidence has suggested that zeolite nucleation does not occur strictly in the solution phase as one might imagine from classical nucleation concepts, but that amorphous particles form even in »clear« aluminosilicate solutions, and that the reconstruction to form crystalline material, the »nuclei«, occurs inside the amorphous particles.[26] Since the nuclei (particles of quasicrystalline phase)[36] cannot grow inside the gel matrix,[43] they are potential nuclei when they are »hidden« in the gel matrix and can start to grow after their »release« from the gel dissolved during the crystallization, *i.e.*, when they are in full contact with the liquid phase (autocatalytic nucleation).[5,7–9,17,21,22,28,33,44,45] Analysis of many kinetics of crystallization of different types of zeolites gave rise to the idea of autocatalytic nucleation.[5,7–9,17,21,22,28,32,33,41,44–49] Hence, the rate of autocatalytic nucleation, and thus the rate of crystallization, as well as the particulate properties of the crystalline end products, depend on the rate of gel dissolution and the number and distribution of the particles of quasicrystalline phase (nuclei) inside the gel matrix.[9,47–49]

Based on these findings and on the preliminary study of the »memory« effect of aluminosilicate gel precursors, namely that the rates of nucleation, crystal growth and crystallization largely depend on the gel pretreatment and crystallization conditions, but that these factors do not affect particulate properties of the crystalline end products,[50] it can be postulated that a real rate of zeolite nucleation depends on the number and distribution of the particles of quasicrystalline phase in the gel matrix as well as on the rates of gel dissolution and zeolite crystal growth (*i.e.*, on the crystallization conditions), but that the particulate properties of the crystalline end products depend exclusively on the number and distribution of the particles of quasicrystalline phase in the gel matrix.

This postulation will be substantiated in the current investigation of the »memory« effect of aluminosilicate gel precursors in three ways: (i) by simulation of the crystallization of zeolites under various conditions, from the gel having a defined number and distribution of nuclei (particles of quasicrystalline phase), (ii) by analysis of the corresponding kinetic data from appropriate literature, and (iii) by analysis of the relevant data obtained from the specially designed kinetic experiments of zeolite crystallization. The aim of this work is to demonstrate the »memory« effect of amorphous aluminosilicate gels by simulation of zeolite crystallization from the gels under various conditions, using the population balance method.

PRINCIPLES OF SIMULATION AND DATA ANALYSIS

Model System

An aluminosilicate hydrogel having the batch molar composition: 4.08 $Na_2O \cdot Al_2O_3 \cdot 1.93\ SiO_2 \cdot 170\ H_2O$, and containing 78.8 g (= m_G^o) of precipitate (solid amorphous aluminosilicate having the molar composition: $Na_2O \cdot Al_2O_3 \cdot 2.106\ SiO_2 \cdot 1.5\ H_2O$) dispersed in 960.6 ml of the solution containing 2 mol dm^{-3} Na (= $c_{Na}(0)$), 0.1 mol dm^{-3} Al (= $c_{Al}(0)$) and 0.0509 mol dm^{-3} Si (= $c_{Si}(0)$) was used as the starting model system.

Heating of the hydrogel at appropriate temperature(s), 78.8 g of the solid amorphous aluminosilicate (gel) having the molecular mass M_G = 317.54 g mol^{-1} and containing 2 moles Al (= x) and 2.106 moles of Si (= y), respectively, per one mole (317.54 g) of the gel, transforms to 99.071 g (= m_z(eq)) of zeolite A ($Na_2O \cdot Al_2O_3 \cdot 2\ SiO_2 \cdot 4.5\ H_2O$) having the molecular mass M_Z = 365.11 g mol^{-1} and containing 2 moles Al (= z_1) and 2 moles of Si (= z_2), respectively, per one mole (365.11 g) of zeolite A.

The equilibrium concentrations, c_{Al}(eq) = 0.052 mol dm^{-3} of aluminum and c_{Si}(eq) = 0.03 mol dm^{-3} of silicon in the liquid phase at the end of the crystallization process (complete transformation of the amorphous aluminosilicate gel to zeolite A) are determined by the batch composition and distribution of Na, Al and Si between the solid and the liquid phase of the starting aluminosilicate hydrogel as well as by the concentrations $c_{Al}^* = c_{Si}^*$ = 0.03 mol dm^{-3} of aluminum and silicon, respectively, in the liquid phase, corresponding to the solubility of zeolite at given crystallization conditions.

Changes of the characteristic parameters (the fraction, f_Z, of zeolite A crystallized, the concentrations, c_{Al}, of aluminum and c_{Si}, of silicon in the liquid phase, the size, L_m, of the largest zeolite crystals and the rate, dN/dt_C, of nucleation) during the crystallization of zeolite A from the model aluminosilicate hydrogel under different conditions were simulated by the population balance method, using the appropriate mechanisms of gel dissolution, formation of primary zeolite particles (nucleation) and their crystal growth.

Population Balance of Zeolite Crystallization

Among different models of zeolite crystallization, only population balance models are based on the fundamental theories of particulate processes that occur during crystallization.[13,15,17,49,51–53] Hence, the population balance methodology enables the simulation of crystallization processes using different mechanisms of gel dissolution, and nucleation and crystal growth of zeolite particles.

The population balance for zeolite crystallization in a well mixed, isothermal, constant volume batch crystallizer, *i.e.* under the conditions characteristic of most zeolite syntheses, may be defined by a set of ordinary differential equations,[17,52] *viz.*

$$\mathrm{d}m_o/\mathrm{d}t_c = \mathrm{d}N/\mathrm{d}t_c = B \tag{1}$$

$$\mathrm{d}m_1/\mathrm{d}t_c = m_o k_g (c_{Al} - c_{Al}^*)\,(c_{Si} - c_{Si}^*)^r \tag{2}$$

$$\mathrm{d}m_2/\mathrm{d}t_c = 2m_1 k_g (c_{Al} - c_{Al}^*)\,(c_{Si} - c_{Si}^*)^r \tag{3}$$

$$\mathrm{d}m_3/\mathrm{d}t_c = 3m_2 k_g (c_{Al} - c_{Al}^*)\,(c_{Si} - c_{Si}^*)^r \tag{4}$$

$$\mathrm{d}L/\mathrm{d}t_c = k_g (c_{Al} - c_{Al}^*)\,(c_{Si} - c_{Si}^*)^r \tag{5}$$

$$\mathrm{d}m_G^*/\mathrm{d}t_c = K_S (m_G^o - m_G^*)^{2/3}\,[c_{Al}^*(g) - c_{Al}] \tag{6}$$

$$\mathrm{d}c_{Al}/\mathrm{d}t_c = (xK_S/M_G)\,(m_G^o - m_G^*)^{2/3}\,[c_{Al}^*(g) - c_{Al}] - (3z_1 G\rho m_2\, k_g/M_Z)\,(c_{Al} - c_{Al}^*)\,(c_{S\,i} - c_{Si}^*)^r \tag{7}$$

$$\mathrm{d}c_{Si}/\mathrm{d}t_c = (yK_S/M_G)\,(m_G^o - m_G^*)^{2/3}\,[c_{Al}^*(g) - c_{Al}] - (3z_2 G\rho m_2\, k_g/M_Z)\,(c_{Al} - c_{Al}^*)\,(c_{Si} - c_{Si}^*)^r \tag{8}$$

where,

$$m_i = \int L^i\,(\mathrm{d}N/\mathrm{d}L)\,\mathrm{d}L \tag{9}$$

is i-th (i = 0, 1, 2 and 3) moment of the particle size distribution of zeolite crystals at time t_c, $\mathrm{d}m_o/\mathrm{d}t_c = \mathrm{d}N/\mathrm{d}t_c = B$ is the nucleation rate, $\mathrm{d}L/\mathrm{d}t_c = k_g(c_{Al} - c_{Al}^*)\,(c_{Si} - c_{Si}^*)^r$ is the growth rate of zeolite crystals,[17,48,52] $\mathrm{d}m_G^*/\mathrm{d}t_c = K_S(m_G^o - m_G^*)^{2/3}[c_{Al}^*(g) - c_{Al}]$ is the rate of gel dissolution,[17,53–55] and $\mathrm{d}c_{Al}/\mathrm{d}t_c$ and $\mathrm{d}c_{Si}/\mathrm{d}t_c$ are the rates of changes of the concentration of aluminum and silicon in the liquid phase.[17,52] Here, k_g is the rate constant of the linear, size-independent crystal growth,[56,57] which occurs by a reaction of reactive silicate, aluminate, and/or aluminosilicate species from the liquid phase on the surfaces of the growing zeolite crystals,[43,56,57] K_S is a lumped constant proportional to the dissolution rate constant, m_G^* is the mass of gel dissolved up to the crystallization time t_c, $c_{Al}^*(g)$ is the concentration of aluminum

in the liquid phase corresponding to the solubility of the gel under given crystallization conditions, G and ρ are the geometrical shape factor and density of the growing zeolite crystals, and r is the molar ratio Si/Al of the crystallized zeolite. Meanings of the designations, c_{Al}, c_{Al}^*, c_{Si}, c_{Si}^*, m_G^o, M_G, M_Z, x, y, z_1 and z_2 have been already explained.

According to the model of autocatalytic nucleation of zeolites, the rate of the autocatalytic nucleation may be expressed as:[5,7,9,15,28,41,44–49,53,60]

$$dN/dt_c = F(d)\ (dm_G^*/dt_c) \tag{10}$$

where $F(d)$ is a function of the distribution of nuclei (particles of quasicrystalline phase) in the gel matrix. Based on the analyses of the relationships between the fraction, $(f_G)_L = m_G^*/ m_G^o$, of the gel dissolved during the crystallization and the fraction, $f_N = N/N_o$, of the nuclei »released« from the dissolved amount of gel,[9,47–49,53,60] the general relation between f_N and $(f_G)_L$ may be expressed as,

$$f_N = N/N_o = f_1\{1- \exp[-k_1(f_G)_L]\} + f_2\{1- \exp[-k_2(f_G)_L{}^n]\} \tag{11}$$

where, N_o is the number of nuclei contained in the mass, m_G^o, of the gel, f_1 and f_2 ($f_1 + f_2 = 1$), k_1, k_2 and n are the corresponding constants. Hence, the rate, dN/dt_c , of autocatalytic nucleation is,

$$B = dm_o/dt_c = dN/dt_c = \{f_1\ N_o\ k_1\ \exp[-k_1(f_G)_L] + f_2\ N_o\ k_2(f_G)_L{}^{n-1}\ \exp[-k_2(f_G)_L{}^n]\}\ d(f_G)_L/dt_c \tag{12}$$

where, $\{f_1\, N_o\, k_1 \exp[-k_1(f_G)_L] + f_2\, N_o\, k_2(f_G)_L{}^{n-1} \exp[-k_2(f_G)_L{}^n]\}\ /\ m_G^o = F(d)$.

The effects of the distribution of nuclei in the gel matrix (simulations S1/1 – S1/3), crystal growth rate (simulations S2/1 – S2/3), rate of gel dissolution (simulations S3/1 – S3/3) and crystallization temperature (simulations S4/1 – S4/3) on the system behavior during crystallization of zeolite A under various conditions were simulated by simultaneous solutions of equations (1) – (8) using a fourth-order Runga-Kutta method and the corresponding numerical values of appropriate constants and initial conditions.

Initial Conditions

The following initial conditions (solutions of equations (1) – (8) in $t_c = 0$)[17,52] were used for all simulations:

$m_o(t_c = 0) = N(0)\ L[(0)]^0 = 100 \times (10^{-6})^0 = 100$

$m_1(t_c = 0) = N(0)\ L[(0)]^1 = 100 \times (10^{-6})^1 = 10^{-4}$ cm

$m_2(t_c = 0) = N(0)\ L[(0)]^2 = 100 \times (10^{-6})^2 = 10^{-10}$ cm^2

$m_3(t_c = 0) = N(0)\ L[(0)]^3 = 100 \times (10^{-6})^3 = 10^{-16}$ cm^3

$L(t_c = 0) = 10^{-6}$ cm

$m_G^*(t_c = 0) = 0$

$c_{Al}(t_c = 0) = 0.1$ mol dm^{-3}

$c_{Si}(t_c = 0) = 0.0509$ mol dm^{-3}.

Input Data (Constants)

$c_{Al}^*(g) = 0.1$ mol dm^{-3} for all simulations

$c_{Al}^* = c_{Si}^* = 0.03$ mol dm^{-3} for all simulations

$f_1 = 0.8$, $f_2 = 0.2$ for simulation S1/3; $f_1 = 1$, $f_2 = 0$ for all other simulations

$G = 1$ (cubes) for all simulations

$k_1 =$ 25 for simulation S1/1; $k_1 = 15$ for simulation S1/3; $k_1 = 10$ for all other simulations

$k_2 = 1000$ for simulation S1/3

$k_g =$ 0.324 cm mol^{-2} dm^6 h^{-1} for simulation S4/1; $k_g = 0.25$ cm mol^{-2} dm^6 h^{-1} for simulation S2/1; $k_g = 0.5$ cm mol^{-2} dm^6 h^{-1} for simulations S1/1 – S1/3, S2/2, S3/1 – S3/3 and S4/2; $k_g = 0.75$ cm mol^{-2} dm^6 h^{-1} for simulation S2/3, and $k_g = 0.754$ cm mol^{-2} dm^6 h^{-1} for simulation S4/3

$K_S =$ 250 g$^{1/3}$ mol^{-1} dm^3 h^{-1} for simulation S3/1; $K_S = 864$ g$^{1/3}$ mol^{-1} dm^3 h^{-1} for simulation S4/1; $K_S = 1000$ g$^{1/3}$ mol^{-1} dm^3 h^{-1} for simulations S1/1 – S1/3, S2/1 – S2/3, S3/2 and S4/2; $K_S = 1149$ g$^{1/3}$ mol^{-1} dm^3 h^{-1} for simulation S4/3 and $K_S = 3000$ g$^{1/3}$ mol^{-1} dm^3 h^{-1} for simulation S3/3.

$m_G^o = 78.8$ g for all simulations

$M_G = 317.54$ g mol^{-1} for all simulations

$M_Z = 365.11$ g mol^{-1} for all simulations

$N_o = 9.456 \times 10^{11}$ for all simulations

$n = 5$ for simulation S1/3; $n = 0$ for all other simulations

$\rho = 2$ g cm^{-3} for all simulations

$x = 2$ for all simulations

$y = 2.106$ for all simultions

$z_1 = z_2 = 2$ for all simulations.

Data Output (Results)

The values of $L = L_m$ (size of the largest zeolite crystals), c_{Al} and c_{Si} at any crystallization time, t_c, were obtained in a direct way as appropriate solutions of Eqs. (5), (7) and (8), respectively. The values, $f_Z = m_Z / (m_Z + m_G)$, where m_Z is the mass of crystallized zeolite and m_G is the mass of the untransformed gel were calculated as:[17,52]

$$f_Z = G\rho m_3 / (G\rho m_3 + m_G^o - m_G^*) \quad (13)$$

where m_3 is the third moment of distribution, proportional to the mass of crystallized zeolite and obtained by the solution of Eq. (4) for the time of crystallization, t_c, and m_G^* is the mass of the gel dissolved up to time t_c, and obtained by the solution of Eq. (6) for the same time of crystallization. The rates of nucleation, dN/dt_c, were calculated by a combination of Eqs. (6) and (12):

$$dN/dt_c = K_S(m_G^o - m_G^*)^{2/3} \left[c_{Al}^*(g) - c_{Al}\right] \{f_1 N_o k_1 \exp(-k_1 m_G^*/m_G^o) + f_2 N_o k_2 (m_G^*/m_G^o)^{n-1} \exp[-k_2 (m_G^*/m_G^o)^n]\} \quad (14)$$

Here, the values of m_G^* and c_{Al} represent the solutions of Eqs. (6) and (7), respectively, for a given crystallization time t_c.

The crystal size distributions of the crystalline end product were calculated from the nucleation and crystal growth data by the method proposed by Zhdanov.[5,29]

RESULTS AND DISCUSSION

The first step of our analysis was to show how the distribution of nuclei (particles of quasicrystalline phase) in the gel matrix influences the critical processes of zeolite crystallization and the particulate properties of the crystalline end product. For this purpose, three different distributions of nuclei in the gel matrix were simulated by Eq. (11), using the relevant values of f_1, f_2, k_1, k_2 and n (see *Data Input*), and presented in Figure 1 as the fractions, f_N, of the nuclei »released« from the part (fraction), $(f_G)_L$, of the gel dissolved during crystallization.

Figure 2 shows the results of simulations S1/1 (solid curves), S1/2 (dashed curves) and S1/3 (dotted curves) of zeolite A crystallization under

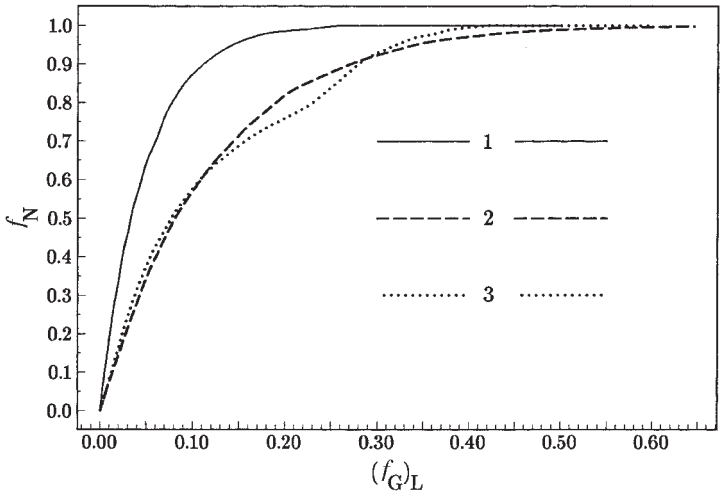

Figure 1. Distribution of nuclei in the gel matrix, presented as fractions, f_N, of the nuclei »released« from the part (fraction, $(f_G)_L$), of gel dissolved during crystallization. Distributions of nuclei in gel-1 (solid curve), gel-2 (dashed curve) and gel-3 (dotted curve) are simulated by Eq. (11) and the relevant values of the corresponding constants (see *Input Data*).

identical conditions, from three gels characterized by specific distribution of nuclei (see Figure 1).

The changes of fractions, f_Z, of the crystallized zeolite (Figure 2A), concentrations, c_{Al} of aluminum and, c_{Si}, of silicon, in the liquid phase (Figure 2B), dimensions, L_m, of the largest zeolite crystals (Figure 2C) and the rates, dN/dt_c, of autocatalitic nucleation (»releasing« of nuclei from the dissolved gel) (Figure 2D) during the crystallization, are typical of most zeolite syntheses.[1,3,4–10,15,17,28,29,44–48] The results presented in Figure 2 show that the changes in f_Z, c_{Al}, c_{Si}, dN/dt_c, and even L_m (at least at the end of the crystallization process) during the crystallization of zeolite A from three different gels, under the same conditions (see *Initial Conditions* and *Data Input*) considerably depend on the gel properties specified by the distribution of the constant number, N_o, of the particles of quasicrystalline phase (nuclei) in the gel matrix (see Figure 1). As expected, the rate of crystallization is the highest during the transformation of gel-1 (simulation S1/1; solid curves in Figure 2) due to the most expressive inhomogeneity in the distribution of nuclei in this gel (solid curve in Figure 1), *i.e.*, $dN/d(f_G)_L$ (gel-1) > $dN/d(f_G)_L$ (gel-2; dashed curve in Figure 1) ≅ $dN/d(f_G)_L$ (gel-3; dotted curve in Figure 1) during the initial stage of gel dissolution ($(f_G)_L > 0.2$), in which most of the nuclei are »released« from the gel matrix (compare Figures 1A and 1D). For

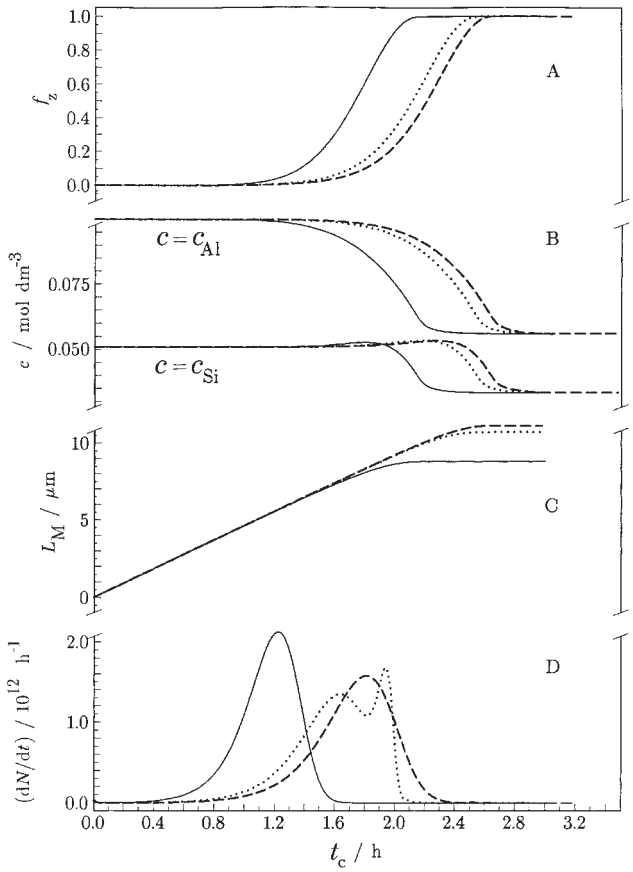

Figure 2. Change in: (A) fractions, f_Z, of zeolite crystallized, (B) concentrations of aluminum, c_{Al} and of silicon, c_{Si}, (C) dimension, L_M, of the largest zeolite crystals and (D) rate of nucleation (»release« of the particles of quasicrystalline phase from the dissolved gel), dN/dt_c, during crystallization of zeolite A from gels 1, 2 and 3 (see Figure 1), obtained as the results of simulations S1/1 (solid curves), S1/2 (dashed curves) and S1/3 (dotted curves).

the same reason, the specific changes obtained by simulation S1/2 (transformation of gel-2; dashed curves in Figures 1 and 2) and S1/3 (transformation of gel-3; dotted curves in Figures 1 and 2) do not differ considerably. The appearance of two maxima in the nucleation curve obtained in simulation S1/3 (dotted curve in Figure 2D) is caused by a specific »two-step« distribution of nuclei in gel-3 (dotted curve in Figure 1). Figure 3 shows the crystal size distribution curves of the crystalline end products obtained by crystallization of zeolite A from gels 1 (simulation S1/1; solid curve), 2 (simulation S1/2; dashed curve), and 3 (simulation S1/3; dotted curve).

Although there is no doubt that the crystal size distribution of the crystalline end product depends on the rate of nucleation,[5,9,13,15,48,49,60] and thus in accordance with the model of autocatalytic nucleation on the distribution of nuclei in the gel matrix[9,49,50,60] (see also Eqs. (10) and (11)), the real influence of these factors as well as of other relevant processes (rate of gel dissolution, rate of crystal growth) on the crystal size distribution in the crystalline end product cannot be estimated only on the basis of the present data. For this reason, the next step of our analysis includes simulations of zeolite crystallization from a gel with a defined number and distribution of nuclei; gel-2 (dashed curves in Figure 1) is used as the reference precursor, under different conditions. The crystallization conditions were determined by the change of the growth rate constant, k_g (simulations S2/1, S2/2 and S2/3), constant, K_S, of the gel dissolution (simulation S3/1, S3/2 and S3/3) and the simultaneous change of constants k_g and K_S by the change of crystallization temperature T_c (simulations S4/1, S4/2 and S4/3).

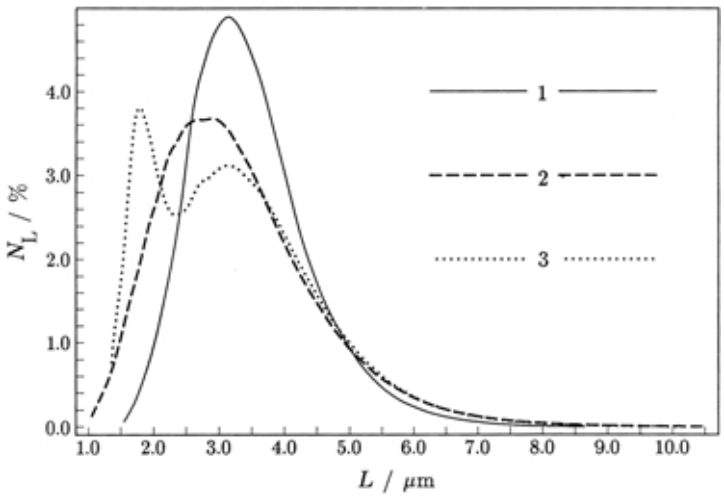

Figure 3. Crystal size distribution curves of the crystalline end products obtained by zeolite A crystallization from gels 1 (simulation S1/1; solid curve), 2 (simulation S1/2; dashed curve) and 3 (simulation S1/3; dotted curve).

The rate of linear growth of zeolite crystals is directly proportional to the product of the growth rate constant, k_g, and the concentration factor, $f(c) = (c_{Al} - c_{Al}^*)\,(c_{Si} - c_{Si}^*)^r$ (see Eq. (5)).[17,52,54] Hence, the rate of linear crystal growth influences, in a direct way, the rates of the particulate processes (see the moment Eqs. (2), (3) and (4)), and in a indirect way (through the chan-

ges in concentrations, c_{Al}, of aluminum and, c_{Si}, of silicon in the liquid phase) the rates of gel dissolution (see Eq. (6)) and nucleation (see Eqs. (10), (12) and (14)), as well as the changes in concentrations, c_{Al}, of aluminum (see Eq. (7) and, c_{Si}, of silicon (see Eq. (8)) in the liquid phase during crystallization. In a real case, the rate of crystal growth may be controlled by controlling both the concentration factor, $f(c)$ (*e.g.*, increase of $f(c)$ by the increase of gel solubility with increasing alkalinity of the liquid phase,[58] or decrease of $f(c)$ by dilution of the liquid phase) and the value of the growth rate constant, k_g (*e.g.*, increase of the value of k_g by the increase of crystalli-

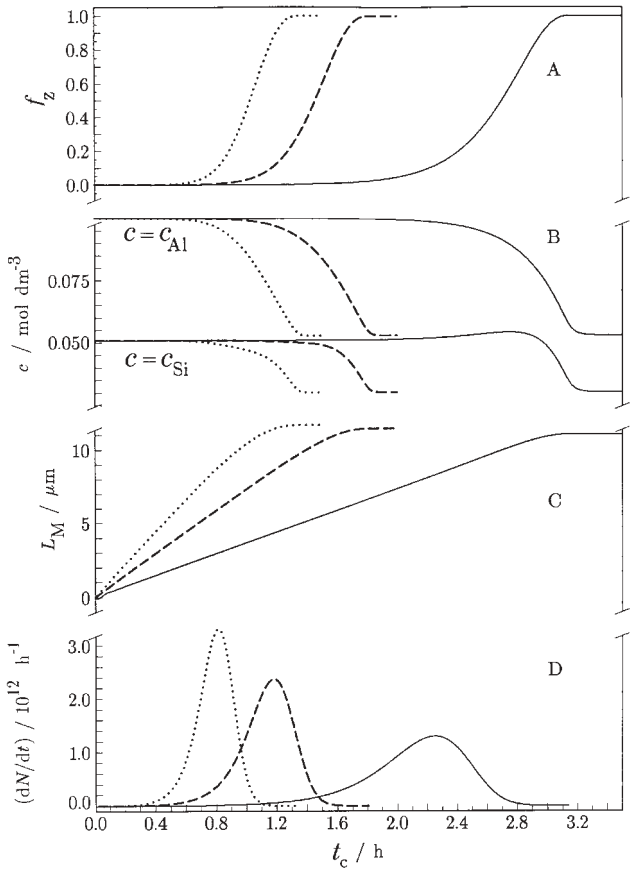

Figure 4. Change in: (A) fractions, f_Z, of zeolite crystallized, (B) concentrations of aluminum, c_{Al}, and of silicon, c_{Si}, (C) dimension, L_M, of the largest zeolite crystals, and (D) rate of nucleation (»release« of the particles of quasicrystalline phase from the dissolved gel), dN/dt_c, during zeolite A crystallization from gel-2 (dashed curve in Figure 1), obtained as the results of simulations S2/1 (solid curves), S2/2 (dashed curves) and S2/3 (dotted curves).

zation temperature,[5,49] or decrease of the value of k_g caused by the presence of K^+ ions in the liquid phase of the system).[29,61] For simplicity, the crystal growth rate in simulations S2/1, S2/2 and S2/3 was controlled by the value of the growth rate constant, k_g; the values, k_g = 0.25 cm mol^{-2} dm^6 h^{-1} (simulation S2/1), k_g = 0.5 cm mol^{-2} dm^6 h^{-1} (simulation S2/2) and k_g = 0.75 cm mol^{-2} dm^6 h^{-1} (simulation S2/3) were used for this purpose. Figure 4 shows that an increase of the crystal growth rate in the proportions, 1 (k_g = 0.25 cm mol^{-2} dm^6 h^{-1}; simulation S2/1; solid curves in Figure 4): 2 (k_g = 0.5 cm mol^{-2} dm^6 h^{-1}; simulation S2/2; dashed curves in Figure 4): 1.5 (k_g = 0.75 cm mol^{-2} dm^6 h^{-1}; simulation S2/3; dashed curves in Figure 4) considerably increases the rate of nucleation (Figure 4D), rate of gel dissolution, $d(f_G)_L/dt_c \approx df_Z/dt_c$, changes in concentrations, c_{Al}, of aluminum and, c_{Si}, of silicon in the liquid phase (Figure 4B) and the rate of entire crystallization process (Figure 4A) during the crystallization of zeolite A from the gel with a constant number and distribution, respectively, of the particles of quasicrystalline phase (gel-2; dashed curve in Figure 1) at constant temperature (80 °C) and under other constant conditions (see *Input Data*).

The influence of the crystal growth rate on other relevant critical processes of zeolite crystallization is in agreement with theoretical considerations[13–17,47,51–53] and experimental experiences,[1,3,4–10,15,17,28,29,44–48] and hence it will not be additionally discussed here. However, in spite of the considerable differences in the rates of critical processes caused by the differences in the crystal growth rate (see Figure 4), the crystal size distribution of the crystalline end products is not affected either by the rate of crystal growth, or by the rates of other relevant critical processes, *i.e.*, the crystal size distribution in the crystalline end products of all the three simulated crystallization processes (simulations S2/1, S2/2 and S2/3), is almost the same (see Figure 7A).

Figure 5 shows the results of simulations of zeolite A crystallization from the gel with a constant number and distribution, respectively, of the particles of quasicrystalline phase (gel-2; dashed curve in Figure 1) at constant temperature (80 °C) and constant crystal growth rate (k_g = 0.5 cm mol^{-2} dm^6 h^{-1}), but different rates, K_S = 250 g$^{1/3}$ mol^{-1} dm^3 h^{-1}conditions (simulation S3/1; solid curves), K_S = 1000 g$^{1/3}$ mol^{-1} dm^3 h^{-1} (simulation S3/2; dashed curves) and K_S = 3000 g$^{1/3}$ mol^{-1} dm^3 h^{-1} (simulation S3/3: dotted curves), of the gel dissolution.

Although the influence of the rate of gel dissolution on the critical processes of zeolite crystallization is less pronounced than the influence of the crystal growth rate (compare Figures 4 and 5), the increase in the value of the gel dissolution rate constant, K_S, in proportions 1 : 4 : 3, still markedly influences the rate of nucleation (Figure 5D), the changes in the concentra-

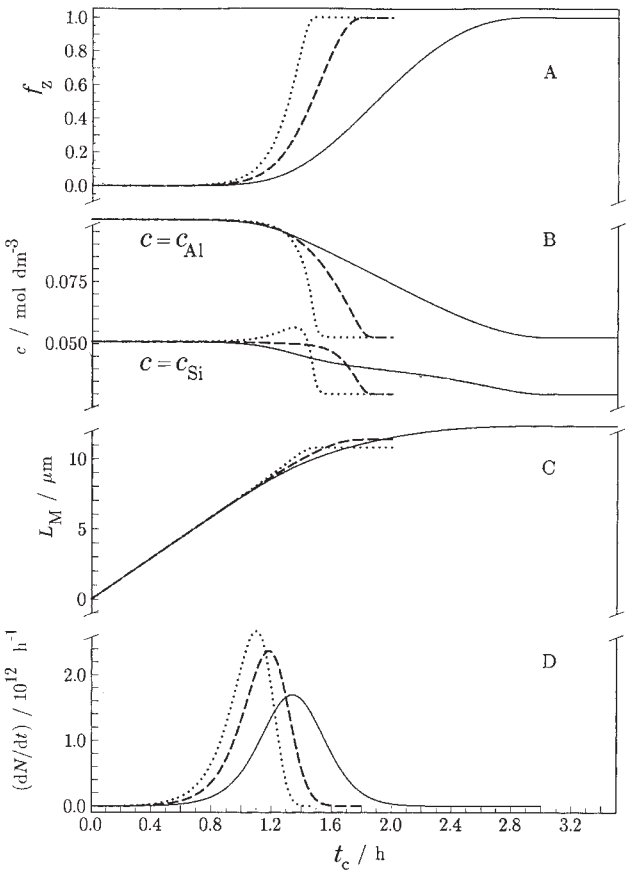

Figure 5. Change in: (A) fractions, f_Z, of zeolite crystallized, (B) concentrations of aluminum, c_{Al}, and of silicon, c_{Si}, (C) dimension, L_M, of the largest zeolite crystals and (D) rate of nucleation (»release« of the particles of quasicrystalline phase from the dissolved gel), dN/dt_c, during zeolite A crystallization from gels-2 (dashed curve in Figure 1), obtained as the results of simulations S3/1 (solid curves), S3/2 (dashed curves) and S3/3 (dotted curves).

tions, c_{Al}, of aluminum and, c_{Si}, of silicon in the liquid phase (Figure 5B), and the rate of the entire crystallization process (Figure 5A); the rate of crystal growth is only slightly influenced by the change in the rate of gel dissolution. Again, the changes in the rates of critical processes, caused by the change in the gel dissolution rate, do not considerably affect the crystal size distribution in the crystalline end products. Moreover, the crystal size distributions in the crystalline end products of the simulated crystallization processes S3/1, S3/2 and S3/3 are almost the same as the crystal size distri-

butions in the crystalline end products of the simulated crystallization processes S2/1, S2/2 and S2/3 (compare Figures 7A and 7B).

Change of the crystallization temperature, T_c, causes a simultaneous change of both the rate of gel dissolution[59] and the rate of crystal growth,[5,28,49] according with the relations,

$$\ln K_S = - E_a(d)/RT_c + \ln A(d) \quad (15)$$

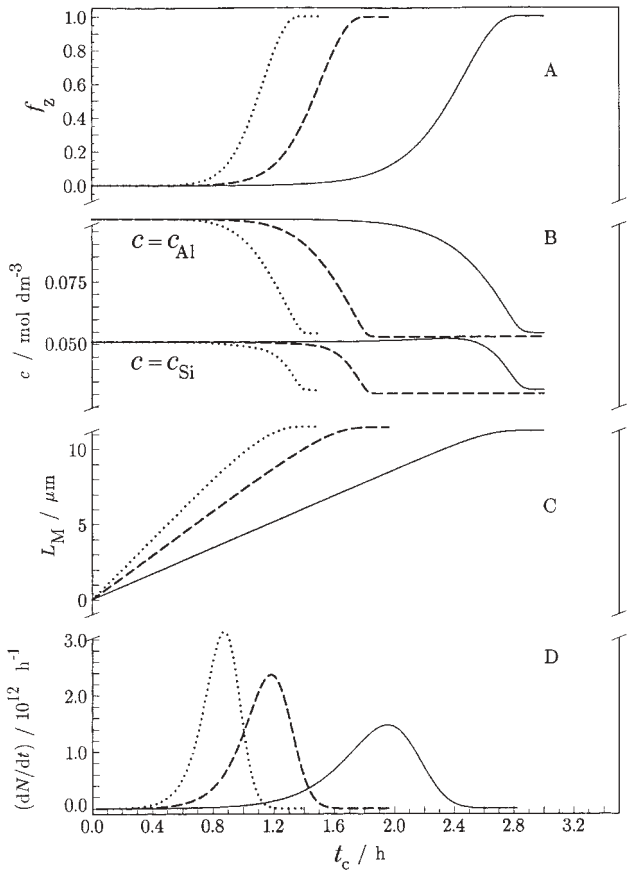

Figure 6. Change in: (A) fractions, f_Z, of zeolite crystallized, (B) concentrations of aluminum, c_{Al}, and of silicon, c_{Si}, (C) dimension, L_M, of the largest zeolite crystals and (D) rate of nucleation (»release« of the particles of quasicrystalline phase from the dissolved gel), dN/dt_c, during zeolite A crystallization from gel-2 (dashed curve in Figure 1), obtained as the results of simulations S4/1 (solid curves), S4/2 (dashed curves) and S4/3 (dotted curves).

$$\ln k_g = - E_a(g)/RT_c + \ln A(g) \quad (16)$$

where $E_a(d) = 14.75$ kJ mol^{-1} is the activation energy of gel dissolution,[59] $E_a(g) = 43.7$ kJ mol^{-1} is the activation energy of the crystal growth of zeolite A,[28] $R = 8.314$ J K^{-1} mol^{-1} is the gas constant, T_c is absolute temperature; ln $A(d) = 11.934$ and ln $A(g) = 14.196$, respectively for conditions: $K_S = 1000$ g$^{1/3}$ mol^{-1} dm^3 h^{-1} and $k_g = 0.5$ cm mol^{-2} dm^6 h^{-1}, for $T_c = 353$ K (80 °C). The values of K_S and k_g, calculated by Eqs. (15) and (15), respectively, were used for simulations of the processes of zeolite A crystallization at different temperatures (70, 80 and 90 °C). Results of the simulation of zeolite A crystalli-

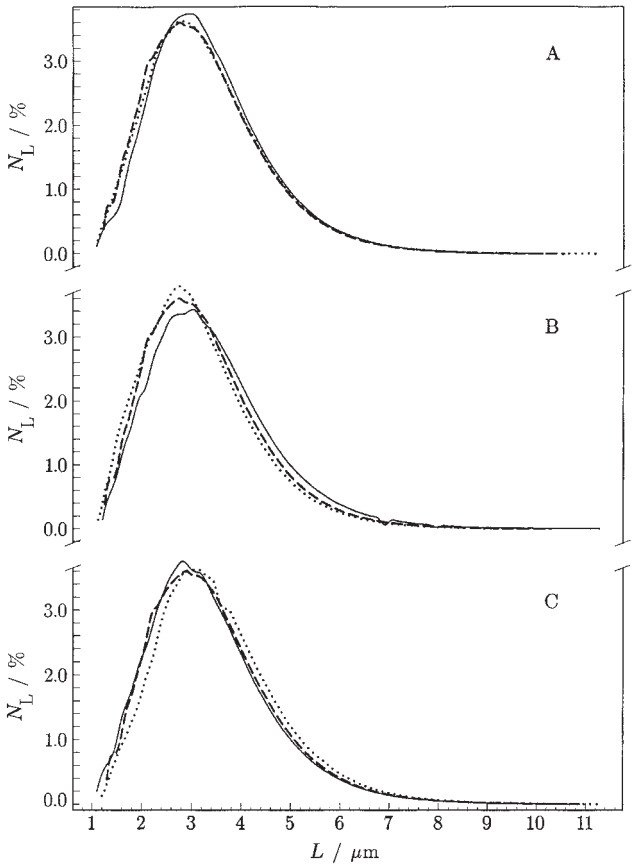

Figure 7. Crystal size distribution of the crystalline end products obtained by: (A) simulations S2/1 (solid curve), S2/2 (dashed curve) and S2/3 (dotted curve), (B) simulations S3/1 (solid curve), S3/2 (dashed curve) and S3/3 (dotted curve), and (C) simulations S4/1 (solid curve), S4/2 (dashed curve) and S4/3 (dotted curve), of the crystallization of zeolite A from gel-2 (dashed curve in Figure 1).

zation at 70 °C (simulation S4/1; solid curves), 80 °C (simulation S4/2; dashed curves) and 90 °C (simulation S4/3; dotted curves) are presented in Figure 6.

As expected, the rates of all relevant critical processes, and thus the overall rate of the crystallization process, increase with the increasing crystallization temperature, T_c, due to the simultaneous increase of the gel dissolution rate and the crystal growth rate, with the increase of the crystallization temperature T_c, but the changes in the rates of critical processes, caused by the change of crystallization temperature, T_c, do not affect the crystal size distribution in the crystalline end products (see Figure 7C). Again, the crystal size distributions in the crystalline end products of the simulated crystallization processes S4/1, S4/2 and S4/3 are almost the same as the crystal size distributions in the crystalline end products of the simulated crystallization processes S2/1, S2/2, S2/3, S3/1, S3/2 and S3/3 (see Figure 7).

CONCLUSION

Results of the simulations of zeolite A crystallization under constant conditions from gels having a constant number and different distributions of nuclei (particles of quasicrystalline phase) in the gel matrix (simulations S1/1, S1/2 and S1/3) have shown that the crystal size distribution of the crystalline end product depends on the rate of nucleation, and thus in accordance with the model of autocatalytic nucleation on the distribution of nuclei in the gel matrix. However, the real influence of these factors as well as of other relevant processes (rate of gel dissolution, rate of crystal growth) on the crystal size distribution in the crystalline end product could not be estimated only on the basis of these data.

Results of the simulations of zeolite A crystallization at different crystal growth rates (simulations S2/1, S2/2 and S2/3), different gel dissolution rates (simulations S3/1, S3/2 and S3/3) and different temperatures (simulations S4/1, S4/2 and S4/3) from the gel having a defined number and distribution of nuclei have shown that changes in crystallization conditions considerably influence the rates of all relevant processes during the crystallization. However, despite the considerable differences in the rates of critical processes, caused by differences in crystallization conditions, the crystal size distribution of the crystalline end products is not affected by the crystallization conditions, and thus by the rates of the relevant critical processes (gel dissolution, nucleation, crystal growth), but only by the number and distribution of the nuclei (particles of quasicrystalline phase) in the gel matrix. Since the particles of the quasicrystalline phase are formed in the

gel matrix during its preparation (precipitation), their number and distribution, in the gel matrix are determined by the conditions and the method of gel preparation. Hence, the crystal size distribution in the crystalline end product is determined by the method and conditions, under which gel is prepared. In other words, it might be expected that the crystal size distribution in the product of crystallization from the gels prepared in the same way, under the same conditions, but hydrothermaly treated under different conditions, would be the same. Constancy of the crystal size distribution in the crystalline end product obtained during the crystallization of zeolite A[27] and zeolite ZSM-5[47] from gels prepared under the same conditions and crystallized at different temperatures supports the thesis of the »memory« effect of gels, here evidenced by the simulation of zeolite crystallization by the population balance method. Experimental evidence of the »memory« effect of gels by detailed analysis of the corresponding kinetic data from appropriate literature and analysis of the proper data obtained from the specially designed kinetic experiments of zeolite crystallization are in progress and will be published elsewhere.

Acknowledgement. – This work was supported by the Ministry of Science and Technology of the Republic of Croatia and by the National Science Foundation (NSF) through mediation of the U.S. – Croatian Joint Board of Scientific and Technological Cooperation.

REFERENCES

1. D. W. Breck, *J. Chem. Educ.* **41** (1964) 678–689.
2. D. E. W. Vaughan, *Chem. Eng. Progr.* (1988) 25–31.
3. R. M. Barrer, *Hydrothermal Synthesis of Zeolites*, Academic Press, London, 1982, p. 105.
4. G. T. Kerr, *J. Phys. Chem.* **72** (1968) 1385–1386.
5. S. P. Zhdanov, *Adv. Chem. Ser.* **101** (1971) 20–43.
6. E. F. Freund, *J. Cryst. Growth* **34** (1976) 11–23.
7. J. Bronić, B. Subotić, I. Šmit, and LJ. A. Despotović, *Stud. Surf. Sci. Catal.* **37** (1988) 107–114.
8. A. Katović, B. Subotić, I. Šmit, and LJ. A. Despotović, *Zeolites* **9** (1989) 45–53.
9. T. Antonić, B. Subotić, and N. Stubičar, *Zeolites* **18** (1997) 291–300.
10. J. Ciric, *J. Colloid Interface Sci.* **28** (1966) 315–324.
11. W. Wieker and B. Fahlke, *Stud. Surf. Sci. Catal.* **24** (1985) 161–181.
12. M. Tassopoulos and R. W. Thompson, *Zeolites* **7** (1987) 243–247.
13. L. M. Truskinovskiy and E. E. Senderov, *Geokhimiya* **3** (1983) 450–461.
14. R. W. Thompson and A. Dyer, *Zeolites* **5** (1985) 202–210.
15. C. L. Huang, W. C. Yu, and T. Y. Lee, *Chem. Eng. Sci.* **41** (1986) 625–32.
16. J. D. Cook and R. W. Thompson, *Zeolites* **8** (1988) 322–326.

17. B. Subotić and J. Bronić, in: R. von Ballmoos, J. B. Higgins, and M. J. M. Treacy (Eds.), *Proceedings of the 9th International Zeolite Conference,* Montreal, Canada, 1992, Butterworth-Heinemann, Boston, 1992, pp. 321–328.
18. J. B. Nagy, P. Bodart, H. Collette, C. Fernandez, Z. Gabelica, A. Nastro, and R. Aiello, *J. Chem. Soc., Faraday Trans. 1* **85** (1989) 2749–2769.
19. R. D. Edelman, V. Dinesh, V. Kudalkar, T. Ong, J. Warzywoda, and R. W. Thompson, *Zeolites* **9** (1989) 496–502.
20. J. Warzywoda, R. D. Edelman, and R. W. Thompson, *Zeolites* **11** (1991) 318–324.
21. G. Golemme, A. Nastro, J. B. Nagy, B. Subotić, F. Crea, and R. Aiello, *Zeolites*, **11** (1991) 776–783.
22. E. Narita, K. Sato, N. Yatabe, and T. Okabe, *Ind. Eng. Chem. Prod. Res. Dev.* **24** (1985) 507–512.
23. B. J. Schoeman, J. Sterte, and J.-E. Otterstedt, *J. Porous Mater.* **1** (1995) 185–198.
24. B. J. Schoeman, J. Sterte, and J.-E. Otterstedt, *J. Colloid Interface Sci.* **170** (1995) 449–456.
25. G. S. Wiersema and R. W. Thompson, *J. Mater. Chem.* **6** (1996) 1693–1699.
26. L. Gora, K. Streletzky, R. W. Thompson, and G. D. J. Phillies, *Zeolites* **18** (1997) 119–131.
27. J. Bronić and B. Subotić, *Microporous Materials* **4** (1995) 239–242.
28. S. P. Zhdanov and N. N. Samulevitch, in: L. V. C. Rees (Ed.), *Proceedings of the 5th International Zeolite Conference,* Naples, Italy, 1980, Heyden, London-Philadelphia- -Rheine, 1980, pp. 75–84.
29. W. Meise and F. E. Swochow, *Adv. Chem. Ser.* **121** (1973) 169–178.
30. F. Polak and A. Cichocki, *Adv. Chem. Ser.* **121** (1973) 209–216.
31. H. Lechert, in: P. A. Jacobs (Ed.), *Structure and Reactivity of Modified Zeolites*, Elsevier, Amsterdam, 1984, pp. 107–123.
32. G. Seo, *Hwakak Konghak* **23** (1985) 295–301.
33. A. Katović, B. Subotić, I. Šmit, LJ. A. Despotović, and M. Ćurić, *ACS Symp. Ser.* **398** (1989) 124–139.
34. R. Mostowicz and L. B. Sand, *Zeolites* 3 (1983) 219–225.
35. Z. Gabelica, N. Blom, and E. G. Derouane, *Appl. Catal.* **5** (1983) 227–248.
36. L. A. Bursill and J. M. Thomas, in: R. Sersale, C. Collela, and R. Aiello (Eds.), *Recent Progress Report and Discussions: 5th International Zeolite Conference*, Naples, Italy, 1980, Giannini, Naples, 1981, pp. 25–30..
37. G. Engelhardt, B. Fahlke, M. Mägi, and E. Lippmaa, *Zeolites* **3** (1983) 292.
38. T. Ito, J. Fraissard, J. B. Nagy, N. Dewaele, Z. Gabelica, A. Nastro, and E. G. Derouane, *Stud. Surf. Sci. Catal.* **49** (1989) 579–588.
39. O. Okamura, Y. Tsuruta, and T. Satoh, *Gypsum and Lime* **206** (1987) 23–28.
40. R. Aiello, F. Crea, A. Nastro, B. Subotić, and F. Testa, *Zeolites* **11** (1981) 767–775.
41. B. Subotić, A. M. Tonejc, D. Bagović, A. Čižmek, and T. Antonić, *Stud. Surf. Sci. Catal.* **84A** (1984) 259–266.
42. M. D. Richards and C. G. Pope, *J. Chem. Soc., Faraday Trans.* **92** (1996) 317–323.
43. H. Kacirek and H. Lechert, *J. Phys. Chem.* **79** (1975) 1589–1595.
44. B. Subotić and A. Graovac, *Stud. Surf. Sci. Catal.* **24** (1985) 199–206.
45. B. Subotić, *ACS Symp. Ser.* **398** (1989) 110–123.
46. S. Gonthier, L. Gora, I. Güray, and R. W. Thompson, *Zeolites* **13** (1993) 414–418.
47. S. Gonthier and R. W. Thompson, *Stud. Surf. Sci. Catal.* **85** (1994) 43–73.

48. B. Subotić, T. Antonić, I. Šmit, R. Aiello, F. Crea, A. Nastro, and F. Testa, in: M. L. Occelli and H. Kessler (Eds.), *Synthesis of Porous Materials: Zeolites, Clays and Nanostrucures,* Marcel Dekker Inc., New York-Basel-Hong Kong, 1996, pp. 35–58.
49. C. Falamaki, M. Edrissi, and M. Sohrabi, *Zeolites* **19** (1987) 2–5.
50. T. Antonić and B. Subotić, in: *Zeolite Synthesis: From Dream to Production,* Scientific Program and Abstracts of the 1st EUROWOKSHOP on Zeolites, Ronce-Les-Bains (La Rochelle), France, March 17–20, 1996, p. 33.
51. R. W. Thompson and A. Dyer, *Zeolites* **5** (1985) 292–301.
52. J. Bronić, Ph.D. Thesis, University of Zagreb, 1992.
53. A. Y. Skeikh, A. G. Jones, and P. Graham, *Zeolites* **16** (1996) 164–172.
54. E. Grujić, B. Subotić, and LJ. A. Despotović, *Stud. Surf. Sci. Catal.* **49A** (1989) 261–270.
55. T. Antonić, A. Čižmek, C. Kosanović, and B. Subotić, *J. Chem. Soc., Faraday Trans.* **89** (1993) 1817–1822
56. T. Antonić, A. Čižmek, and B. Subotić, *J. Chem. Soc., Faraday Trans.* **89** (1993) 1973–1977.
57. R. M. Barrer, *Hydrothermal Synthesis of Zeolites*, Academic Press, London, 1982, p. 133.
58. B. J. Schoeman, J. Sterte, and J.-E. Otterstedt, *Zeolites* **14** (1994) 568–575.
59. T. Antonić, A. Čižmek, and B. Subotić, *J. Chem. Soc., Faraday Soc.* **90** (1994) 3725–3728.
60. R. W. Thompson, in: C. R. A. Catlow (Ed.), *Modeling of Structure and Reactivity of Zeolites,* Academic Press, London, 1992, pp. 231–255.
61. J. Warzywoda and R. W. Thompson, *Zeolites* **11** (1991) 577–582.

SAŽETAK

Dokazivanje učinka »pamćenja« amorfnih alumosilikatnih gelova simulacijom procesa kristalizacije zeolita metodom populacijske ravnoteže

Tatjana Antonić i Boris Subotić

Postoje mnogi eksperimentalni dokazi da najveći dio, ili čak svi nukleusi zeolita nastaju u alumosilikatnom gelu i/ili međupovršini između čestica gela i tekuće faze, povezivanjem specifičnih strukturnih jedinica tijekom taloženja i/ili starenja gela. Budući da takvi nukleusi (čestice kvazikristalne faze) ne mogu rasti u matrici gela, oni predstavljaju potencijalne nukleuse koji počinju rasti tek nakon »oslobađanja« iz gela otopljenog tijekom kristalizacije, t.j. kada su u punom kontaktu s tekućom fazom (autokatalitička nukleacija). Na osnovi takvih saznanja zaključeno je da brzina autokatalitičke nukleacije ovisi o brzini otapanja gela te o broju i raspodjeli nukleusa u matrici gela. Međutim, raspodjela veličina kristala u produktu kristalizacije ne ovisi ni o postupku s gelom prije kristalizacije niti o uvjetima kristalizacije, već isključivo o broju i raspodjeli nukleusa u matrici gela. Taj, tzv. učinak »pamćenja« amorfnih alumosilikatnih gelova (prekursora hidrotermalne kristalizacije zeolita) dokazan je simulacijama procesa kristalizacije zeolita pri različitim uvjetima.